Progress In Electromagnetics Research Letters, Vol. 40, 129–139, 2013

CO-DESIGN OF A COMPACT DUAL-BAND FILTER-ANTENNA FOR WLAN APPLICATION

Wei-Jun Wu[1, *], Qi-Feng Liu[1], Qi Zhang[1], and Jing-Ya Deng[2]

[1]Science and Technology on Electromagnetic Compatibility Laboratory, China Ship Development and Design Center, Wuhan 430064, China

[2]School of Science, Xidian University, Xi'an, Shanxi 710071, China

Abstract—A co-designed compact dual-band filter-antenna suitable to be embedded inside a wireless access point (AP) in the 2.45/5.2-GHz wireless local area network (WLAN) bands is presented. The proposed filter-antenna comprises a loop-loaded dual-band monopole radiator and a microstrip dual-band pseudo-interdigital bandpass filter. The monopole consists of a uniform width monopole, two identical capacitively loaded magnetic resonators and a top loaded loop. The two magnetic resonators are loaded at the center of the monopole for dual-band operation and the rectangular loop loaded at the top is involved for miniaturization. Instead of using the traditional $50\,\Omega$ interfaces, the impedance between the filter and antenna is optimized to improve the performance. The filter-antenna and the system circuit board of an AP share the same substrate and ground plane. In this case, the design can fully integrate the circuit board of the AP into an internal filter-antenna solution. The proposed filter-antenna provides good selectivity and rejection in out of band regions and omni-directional radiation patterns within the two desired bands. The measured results show good agreement with the simulated ones.

1. INTRODUCTION

Multifunction, multipurpose components with design of miniaturization are in great demand in wireless communication systems. In these systems, both antennas and filters are usually larger components compared to other components. Thus, it will be of great interest if a single

Received 4 March 2013, Accepted 26 April 2013, Scheduled 26 May 2013

* Corresponding author: Wei-Jun Wu (wj1218wu@126.com).

compact module can be designed to provide both the desired filtering and radiating performances.

There have been several efforts in the literature for integrating the filter and the antenna into a single module. In [1], the patch antenna which consists of four stacked patches exhibits the filtering function. And in [2], the way which can generate filtering performance on the antenna is to cut inverted-L structures on a planar slot antenna. In [3–7], the filter and the antenna are integrated into a single microwave device. For size reduction, pre-designed bandpass filters with suitable configuration have been directly inserted into the feed position of antennas [3–6]. By using an extra impedance transformation structure between the filter and the antenna, the bandpass filter can be integrated properly with the antenna over the required bandwidth [7]. Recently, a co-design approach has been proposed to incorporate the filter and the antenna [8–10]. This integration approach reduces the filter-antenna size and the transmission loss between the filter and the antenna. However, all of these examples mentioned above are single band. The dual-band filter-antenna investigations are relatively few. In [11–13], the dual-band filter and antenna, which have been designed separately with the 50 Ω constraint, are then connected together using 50 Ω transmission line. Because the filter and antenna respective input/output ports are not perfectly matched with the 50 Ω, the impedance bandwidth or selectivity at the input/output port of the filter-antenna is worse.

In this paper, a co-designed compact dual-band filter-antenna for internal AP-filter-antenna applications is presented. The dual-band monopole and dual-band pseudo-interdigital bandpass filter are printed on the same layer, and they share the same ground plane. The filter-antenna substrate and ground plane are the part of the AP's system circuit board. In this case, the design integrates the AP's system circuit board into an internal AP-filter-antenna solution. The uniform width monopole creates the first resonant frequency. Two identical capacitively magnetic resonators are attached to the uniform width monopole. The additional physical resonator structure creates a monopole standing-wave resonance in the second frequency band. A rectangular loop loaded at the top of the monopole is involved for miniaturization. The impedance between the antenna and the filter is optimized to improve the performance of the filter-antenna, without restricting it to 50 Ω. By choosing a proper size for the connected line, the dual bands are matched. Details of the filter-antenna design and the measured results are given. The results show the filter-antenna has good filter performance and radiation characteristics.

2. FILTER-ANTENNA DESIGN

2.1. Dual-band Monopole Design

The geometry of the proposed dual-band monopole is presented in Figure 1(a) along with the design parameters. The antenna is printed on a substrate with $h = 1.0\,\text{mm}$, $\varepsilon_r = 2.65$ and $\tan\delta = 0.001$. It consists of a uniformly wide monopole, two identical capacitively loaded magnetic resonators and a top loaded loop. The loaded top rectangle loop is involved for miniaturization. This novel miniaturization technology uses a below-resonant monopole which possesses a capacitive reactance and a below-resonant loop which has an inductive reactance. The capacitive reactance of the monopole can be cancelled at the reduced resonant frequency by loading an inductive loop. So the inductive loop can match the below-resonant monopole for miniaturization.

Taking into account the current distribution on the monopole, the rectangle loop is selected near the top of the monopole. As the monopole current is maximum at the bottom, the rectangle loop near to the bottom region of the monopole would cause more disturbance to the monopole current in this region. Therefore, the rectangle loop as matching element to the monopole is positioned near the monopole

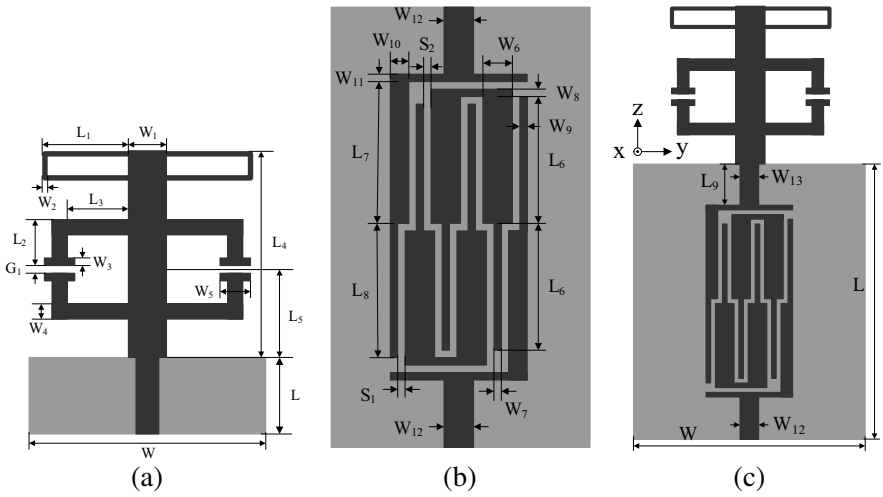

Figure 1. Configuration of the (a) loop-loaded dual-band monopole, (b) dual-band bandpass filter and (c) filter-antenna. Black and gray portions represent the top and bottom metallization, respectively.

top so as to cause minimal interference to the current distributions of monopole. The current on the monopole excites the rectangle loop to induce a magnetic field in the near field region. This compensates the near field capacitive effect generated by the electric field which is produced by the monopole current.

In order to achieve dual-band characteristic, two identical capacitively magnetic resonators are loaded at the center of the monopole. The second frequency band is created by the resonance of the magnetic resonator. The resonant frequency can be adjusted by changing the resonator length $L_2 + L_3$ (modify the inductance), the loop gap G_1, and the strip length W_5 (modify the capacitance).

The optimized design parameters for the monopole with $50\,\Omega$ interface impedance are $W = 34.5\,\text{mm}$, $W_1 = 3\,\text{mm}$, $W_2 = 0.4\,\text{mm}$, $W_3 = 0.4\,\text{mm}$, $W_4 = 1.1\,\text{mm}$, $W_5 = 2.4\,\text{mm}$, $L = 41.5\,\text{mm}$, $L_1 = 7.7\,\text{mm}$, $L_2 = 4.25\,\text{mm}$, $L_3 = 5.1\,\text{mm}$, $L_4 = 17\,\text{mm}$, $L_5 = 7.9\,\text{mm}$, $G_1 = 0.5\,\text{mm}$. The simulated result is shown in Figure 2.

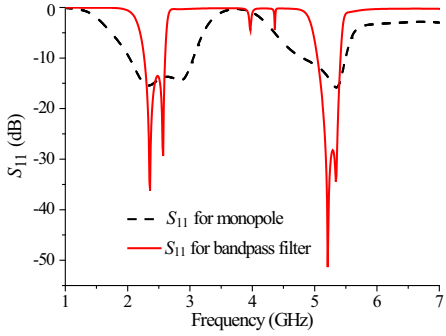

Figure 2. Simulated S_{11} for the monopole and bandpass filter.

2.2. Dual-band BPF Design

Based on the pseudo-interdigital structure and the stepped impedance resonators (SIR), a dual-band bandpass filter (BPF) is proposed in this paper. Figure 3 shows the structure of $\lambda_g/2$ SIR which consists of two transmission lines with impedances Z_1 and Z_2. The resonant condition obtained from input admittance [14, 15], ignoring the effect of step discontinuities is:

$$R_Z = Z_2/Z_1 = \tan\theta_1 \cdot \tan\theta_2 \tag{1}$$

From (1) it is clear that resonant condition for SIR is determined based on θ_1, θ_2 and impedance ratio R_Z. The relationship between

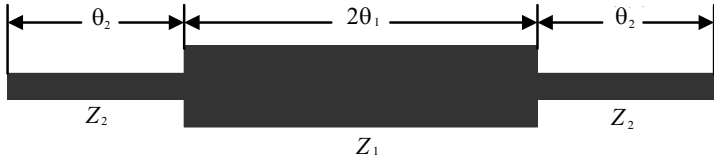

Figure 3. Structure of $\lambda_g/2$ SIR.

fundamental and spurious frequencies is given by

$$\frac{f_{SB}}{f_0} = \frac{\pi}{\tan^{-1}\sqrt{R_z}} - 1 \tag{2}$$

For design of the dual-band bandpass filter, the impedance ratio $R_Z = 2.57$ has been chosen. The lengths $\theta_1 = \theta_2$ are chosen to satisfy the condition of lowest fundamental frequency f_0.

The filter [shown in Figure 1(b)] is printed on a substrate with $h = 1.0\,\text{mm}$, $\varepsilon_r = 2.65$ and $\tan\delta = 0.001$. In our design, the optimized dimensions of the proposed filter are $W_6 = 2.54\,\text{mm}$, $W_7 = 0.34\,\text{mm}$, $W_8 = 0.4\,\text{mm}$, $W_9 = 0.3\,\text{mm}$, $W_{10} = 1.4\,\text{mm}$, $W_{11} = 0.5\,\text{mm}$, $W_{12} = 2.73\,\text{mm}$, $L_6 = 12.1\,\text{mm}$, $L_7 = 13.2\,\text{mm}$, $L_8 = 12.4\,\text{mm}$, $S_1 = 0.3\,\text{mm}$, $S_2 = 0.5\,\text{mm}$. Figure 2 shows the simulated S parameter for the filter.

2.3. Integration

After the designs of antenna and filter separately with the $50\,\Omega$ constraint, the filter-antenna [shown in Figure 1(c)] is implemented. The impedance at the interface of the antenna and the filter is optimized to match the common reference impedance ($50\,\Omega$) in dual bands. Figure 4 shows the effect of varying the width W_{13} of the connected line on the impedance matching of the filter-antenna. It is observed that the upper band is achieved good matching as the width increases, but the lower band is mismatched. So W_{13} is selected to 2 mm to match the dual-band. Figure 5 shows the effect of varying the length L_9 of the connected line on the impedance matching. It is seen that when L_9 is equal to 6 mm, the filter-antenna in the dual bands are both obtained good matching.

3. DISCUSSIONS

In this section, discussions are on the performance of the dual-band monopole, BPF and filter-antenna.

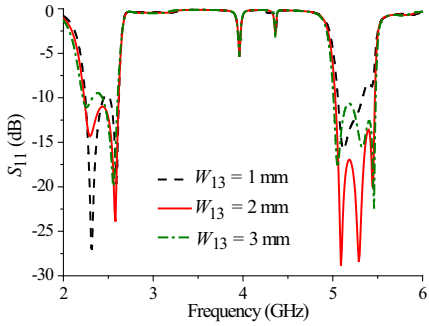

Figure 4. Effect of varying the width W_{13} of the connected line on the impedance matching.

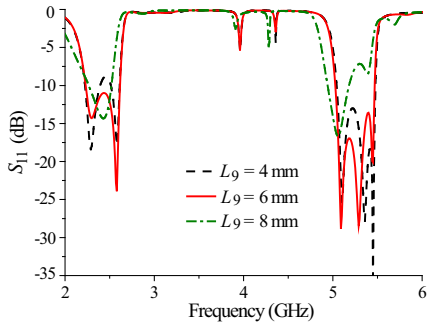

Figure 5. Effect of varying the length L_9 of the connected line on the impedance matching.

3.1. S_{11} of the Dual-band Monopole, BPF and Filter-antenna

Figure 6 shows simulated S_{11} of the dual-band monopole, BPF and filter-antenna. The 10 dB impedance bandwidths of the monopole are 1020 MHz (2.03–3.05 GHz) in the 2.4 GHz band and 690 MHz (4.81–5.5 GHz) in the 5.2 GHz band. The passbands of the BPF are 350 MHz (2.26–2.61 GHz) and 370 MHz (5.04–5.41 GHz). The 10 dB impedance bandwidths of the filter-antenna are 370 MHz (2.24–2.61 GHz) and 430 MHz (5.03–5.46 GHz). From the simulated results, the reflection coefficient of the filter-antenna is dependent on the return loss of the BPF.

3.2. S_{21} of the BPF and Gain of the Monopole and Filter-antenna

Figure 7 shows simulated S_{21} of the BPF and gain of the monopole and filter-antenna in the $+y$ direction. The gain curve of the filter-antenna and the insertion loss curve of the BPF have the similar trend. The filter-antenna has a flat passband response and good frequency skirt selectivity. The simulated gains of the monopole at 1.64, 2.74, 4.69 and 6.18 GHz are 0.06, 0.57, -4.14 and -3.68 dBi, respectively; and the simulated gains of the filter-antenna are -15.45, -20.03, -22.78 and -15.7 dBi. Thus, the filter-antenna has better out-of-band rejection than the monopole, which helps to suppress the noise signal and improve the system performance.

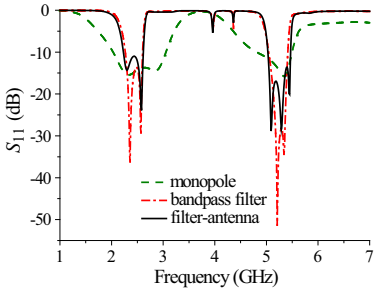

Figure 6. Simulated S_{11} of the monopole, bandpass filter and filter-antenna.

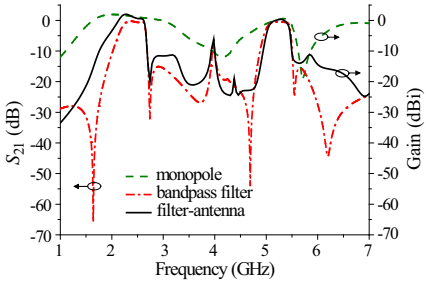

Figure 7. Simulated S_{21} of the bandpass filter and gain of the monopole and filter-antenna.

4. SIMULATED AND MEASURED RESULTS

The proposed filter-antenna has been fabricated and measured. The photograph of the fabricated filter-antenna is shown in Figure 8. To investigate the performance of this filter-antenna, the Ansoft High Frequency Structure Simulator (HFSS.12) simulation software was used for simulations, while the Agilent 8722D vector network analyzer and the Satimo StarLab far field measurement system were used for measurement.

Figure 9 shows simulated and measured S_{11} parameters against frequency of the filter-antenna. According to the measured results, the antenna covers the WLAN 2.4–2.48 GHz and 5.15–5.35 GHz bands easily and provides good selectivity and rejection in out of band

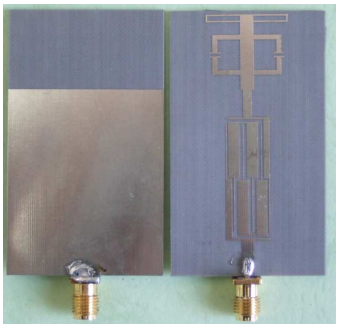

Figure 8. Bottom and top view of the fabricated filter-antenna.

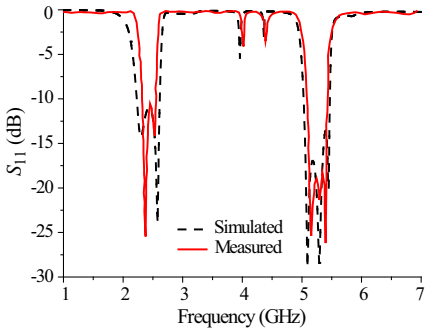

Figure 9. Simulated and measured S_{11} of filter-antenna.

regions. There are two resonances between the two bands, which are created by the spurious resonances of the filter. Three resonances can be seen in the second band. The third resonance is caused by the monopole.

The measured and simulated radiation patterns for the filter-antenna in the x-z and x-y planes at 2.45 and 5.2 GHz are shown in Figure 10. The measured radiation patterns are nearly omni-direction in the azimuth plane in two bands. The gains are about 2.39 and 2.88 dBi at the 2.45 and 5.2 GHz, respectively.

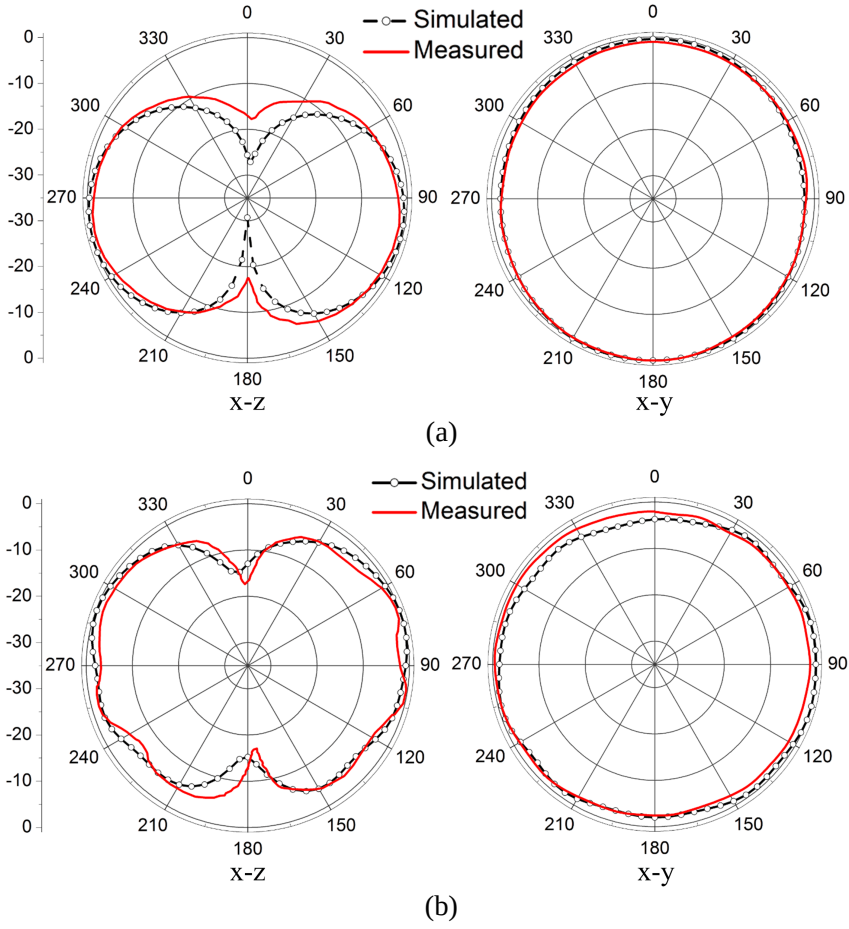

Figure 10. Radiation patterns for the proposed filter-antenna. (a) 2.45 GHz, (b) 5.2 GHz.

5. CONCLUSION

A novel compact loop-loaded monopole with integrated band-select filter for dual-band operation is proposed. The additional physical resonator structure is employed to create the second frequency band. The miniaturization design of a monopole is achieved using a rectangle loop as a reactive loaded element. The reactive loading reduces the resonant frequency of the monopole antenna without affecting the radiation characteristics. The impedance between the antenna and the filter is optimized to improve the performance of the filter-antenna without restricting it to 50 Ω. The filter-antenna provides good selectivity and rejection in out of band regions and omni-directional radiation patterns in dual-band. The proposed design, in this case, integrates the filter-antenna and the AP's system circuit board into a WLAN AP.

REFERENCES

1. Bailey, M.-C., "A stacked patch antenna design with strict bandpass filter characteristics," *IEEE Antennas and Propagation Society International Symposium*, Vol. 2, 1599–1602, Jun. 2004.
2. Barbarino, S. and S. Consoli, "UWB circular slot antenna provided with an inverted-L notch filter for the 5 GHz WLAN band," *Progress In Electromagnetics Research*, Vol. 104, 1–13, 2010.
3. Lee, J.-H., N. Kidera, S. Pinel, J. Laskar, and M.-M. Tentzeris, "Fully integrated passive front-end solutions for a V-band LTCC wireless system," *IEEE Antennas Wireless Propag. Lett.*, Vol. 5, 285–288, 2007.
4. Mandal, M.-K., Z.-N. Chen, and X.-M. Qing, "Compact ultra-wideband filtering antennas on low temperature co-fired ceramic substrate," *Asia Pacific Microwave Conference*, 2084–2087, Dec. 2009.
5. Wong, S.-W., T.-G. Huang, C.-X. Mao, Z.-N. Chen and Q.-X. Chu, "Planar filtering ultra-wideband (UWB) antenna with shorting pins," *IEEE Trans. Antennas Propag.*, Vol. 61, 948–953, 2013.
6. Zhu, Y., F.-S. Zhang, R. Zou, Y.-C. Jiao, and Q.-C. Zhou, "Compact ultra-wideband monopole antenna with novel filter," *Journal of Electromagnetic Waves and Applications*, Vol. 25, Nos. 14–15, 2066–2075, 2011.
7. Troubat, M., S. Bila, M. Thévenot, D. Baillargeat, T. Monédière,

S. Verdeyme, and B. Jecko, "Mutual synthesis of combined microwave circuits applied to the design of a filter-antenna subsystem," *IEEE Trans. Microw. Theory Tech.*, Vol. 55, No. 6, 1182–1189, 2007.

8. Quere, Y., C. Quendo, H.-W. El, and C. Person, "A global synthesis tool and procedure for filter-antenna co-design," *15th International Symposium on Antenna Technology and Applied Electromagnetics*, 1–4, 2012.
9. Wu, W.-J., Y.-Z. Yin, S.-L. Zuo, Z.-Y. Zhang, and J.-J. Xie, "A new compact filter-antenna for modern wireless communication systems," *IEEE Antennas Wireless Propag. Lett.*, Vol. 10, 1131–1134, 2011.
10. Zuo, S.-L., W.-J. Wu, and Z.-Y. Zhang, "A simple filter-antenna with compact size for WLAN application," *Progress In Electromagnetics Research Letters*, Vol. 39, 17–26, 2013.
11. Demir, V., C.-W. P. Huang, and A. Elsherbeni, "Novel dual-band WLAN antennas with integrated band-seltct filter for 802.11 a/b/g WLAN radios in portable devices," *Microwave Opt. Technol. Lett.*, Vol. 49, No. 8, 1868–1872, 2007.
12. Zayniyev, D. and D. Budimir, "Dual-band microstrip antenna filter for wireless communications," *IEEE Antennas and Propagation Society International Symposium (APSURSI)*, 1–4, 2010.
13. Naeem, U., S. Bila, S. Verdeyme, M. Thévenot, and T. Monédière, "A compact dual band filter-antenna subsystem for 802.11 Wi-Fi applications," *Wireless Technology Conference (EuWIT)*, 181–184, 2010.
14. Xu, K.-D., Y.-H. Zhang, C.-L. Zhuge, and Y. Fan, "Miniaturized dual-band bandpass filter using short stub-loaded dual-mode resonators," *Journal of Electromagnetic Waves and Applications*, Vol. 25, No. 16, 2264–2273, 2011.
15. Sagawa, M., M. Makimoto, and S. Yamashita, "Geometrical structures and fundamental characteristics of microwave stepped-impedance," *IEEE Trans. Microw. Theory Tech.*, Vol. 45, No. 7, 1078–1085, 1997.